



Edge-modulated stagnant-lid convection and volcanic passive margins

Norman H. Sleep

Department of Geophysics, Stanford University, Stanford, California 94305, USA (norm@stanford.edu)

[1] The initial oceanic crust along volcanic passive margins is a factor of ~ 3 greater than that of typical oceanic crust (20 versus 6–7 km). Convection driven by the edge of the continental lithosphere may cause mantle material to circulate through the shallow zone of significant melting beneath the nascent ocean basin and cause the volume of melted mantle to exceed that required to replace the diverging lithospheric plates. This hypothesis is a well-known alternative to mantle plumes. I obtain dimensional scaling relations and develop numerical models which indicate that the melted volume is unlikely to be enhanced by a factor of ~ 3 . This conclusion agrees with the results of numerical calculations by Nielsen and Hopper (2002, 2004). Dimensional scaling provides the relationship which shows that the vigor of convection in terms of laterally averaged heat flow (or flow velocity) depends on the square of local thickness of the rheological boundary layer (for linear viscosity). The derivation does not involve undulations in lithospheric thickness and thus provides the inference that the vigor of stagnant-lid convection depends only weakly on those features. Numerical models support this inference. Lithospheric edges do nucleate instabilities, but these instabilities are similar in magnitude to those in models started with a tiny perturbation from laterally homogeneous temperature. Subsequent convection is also similar for models started with tiny perturbations and with large lateral variations in lithospheric thickness. In terms of the scaling relationship, the asthenosphere beneath the thin lithosphere within rifts is an unfavorable site for circulation and extensive melting. The rheological boundary layer is in general thin below thin lithosphere, which causes stagnant-lid convection there to be weak. Care needs to be taken in numerical modeling of convection beneath passive margins. Starting conditions that drive large instabilities of features that could not have persisted in the Earth need to be avoided. Models should start rifting only after mature stagnant-lid convection is established.

Components: 8736 words, 10 figures.

Keywords: volcanic passive margins; stagnant-lid convection; hot spots; mantle plumes; large igneous provinces; lithosphere.

Index Terms: 8105 Tectonophysics: Continental margins: divergent (1212, 8124); 8121 Tectonophysics: Dynamics: convection currents, and mantle plumes; 8120 Tectonophysics: Dynamics of lithosphere and mantle: general (1213).

Received 30 April 2007; **Revised** 21 September 2007; **Accepted** 11 October 2007; **Published** 15 December 2007.

Sleep, N. H. (2007), Edge-modulated stagnant-lid convection and volcanic passive margins, *Geochem. Geophys. Geosyst.*, 8, Q12004, doi:10.1029/2007GC001672.

1. Introduction

[2] Passive margins form when pre-existing continental crust rifts to form a new ocean basin. The thickness of the initial oceanic crust is quite variable. Volcanic margins, including the East Coast of the United States and East Greenland, have oceanic crust on the order of 20 km thick compared to 6–7 km for normal oceanic crust [e.g., *Nielsen and Hopper, 2004; Ernst et al., 2005; Geoffroy, 2005*].

[3] Current hypotheses for forming volcanic passive margins invoke pressure-release melting analogous to mid-oceanic ridge axes. For comparison, material upwells from depth along a melt-free adiabat beneath a fast ridge axis [e.g., *Klein and Langmuir, 1987; Klein, 2003*]. The ascending adiabat intersects the “solidus” where extensive melting begins. Thereafter the material follows a “wet” adiabat where the balance between the latent heat of melting and difference of specific heat between the actual temperature and the melt-free free adiabat determine the temperature. The pooled melts of the ascending column form mid-oceanic ridge basalt (MORB). Three assumptions explain the uniform thickness of crust at most ridges: (1) The temperature (below the region of melting) of the ascending mantle does not vary much. (2) The material ascends monotonically upward. The volume of material that melts is hence that which is required to kinematically replace the lithosphere that moves away from the ridge axis. (3) The composition of the ascending material does not vary greatly with location. Hypothesis for volcanic passive margins postulate that one of the three assumptions for normal ridges is locally inapplicable.

[4] In the mantle plume hypothesis, the assumption of constant source region temperature is inapplicable to volcanic margins. Hot plume material impinges on the base of the lithosphere. This buoyant material flows laterally with the thin lithosphere of the nascent ocean acting as an upside-down drainage pattern for the buoyant plume material (Figure 1a). The hot plume material melts at greater depths than normal mantle and the column yields much more melt. An excess temperature (above the MORB adiabat at great depth) of 200–300 K suffices to produce thickened oceanic crust.

[5] The plume hypothesis has two attractive aspects. Volcanic margins frequently continue into hot spot tracks in the adjacent ocean basin. Buoyant plume material flows laterally so that the

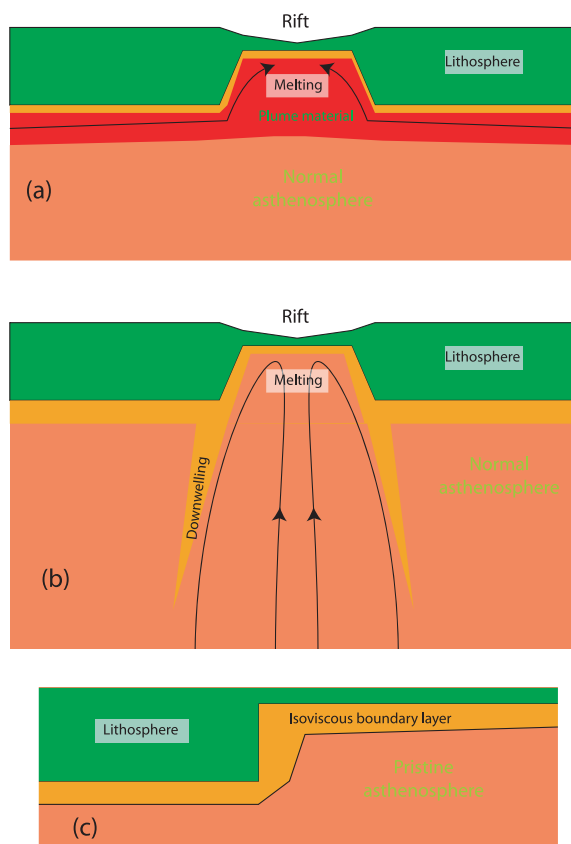


Figure 1. (a) Schematic diagram of plume material flowing into a spreading rift. The hot plume material melts as it arises. Plume material flows in from the sides and along the axis of the rift. The ridge evolves to a normal axis with normal crust when the volume flux from the plume is insufficient to replenish the material carried away from the axis by seafloor spreading. (b) Schematic diagram of vigorous convection beneath a young rift. The rheological boundary layer downwells at the edge of the rift. Much more material circulates through the zone of melting than is kinematically required to replace the material that moves to the sides. The rheological boundary layer is thin beneath thin lithosphere. (c) Schematic diagram of the conditions in numerical models in the works of *King and Anderson [1995, 1998]* and *King [2005]*. The lithosphere has high viscosity, and the asthenosphere has low viscosity. The viscosity boundaries do not evolve with temperature or advect with flow. An isoviscous boundary layer builds up beneath the lithosphere. The edge of the lithosphere nucleates the instability and modulates subsequent flow.

volcanic margins extend far from orifice of their plumes or the center of their starting plume heads.

[6] A second class of explanations postulates that the assumption that flow beneath the rift is monotonically upward is inapplicable (Figure 1b). The

edges of the rift drive convection cooled from above. Mantle material circulates through asthenospheric region beneath the rift. The total amount of melting is thus much greater than that in a single adiabatic column. Here a column with the MORB adiabat produces 6–7 km of crust. To obtain 20-km-thick crust, circulation needs to enhance the total flow by a factor of 3.

[7] A minimum criterion for such edge-driven models is that they evolve to normal constant-thickness oceanic crust after a period of spreading [Nielsen and Hopper, 2002, 2004]. That is, the models must not evolve to vigorous convection beneath mature ridge axes. Neither should the models contain convective instabilities of features that could not have realistically persisted or formed over geological time.

[8] Any edge-driven model for volcanic passive margins faces phenomenological difficulties that make quantification mandatory. One needs to explain why some margins are volcanic and others are starved of melt. In particular, the very slowly spreading Arctic ridge is magma starved [Dick *et al.*, 2003]. The steep relief of the base of the lithosphere on the flanks of this ridge provides edges to drive convection. Ridge jumps and major fracture zones are analogous edges within oceanic lithosphere. They typically do not behave like volcanic passive margins.

[9] The purpose of this paper is to examine the physical effects of relief on the base of the lithosphere on convection cooled from above. To do this, I apply the well-known formalism of stagnant-lid convection. Plumes and plume material are beyond the scope of the paper. So is the detailed petrology and geochemistry of lavas including compositional hypotheses for volcanic margins. The pooled melts from hot plume material should differ from the pooled melts of a circulating column on the MORB adiabat [e.g., Plank *et al.*, 1995]. I begin with a review of the literature with the starting conditions of published numerical models in mind.

2. Previous Work

[10] A large secondary literature utilizes papers that model convection driven by the lithospheric edges beneath rift margins. Nielsen and Hopper [2002, 2004] summarize older works. More recent reviews discuss edge-driven convection as a viable hypothesis [e.g., Geoffroy, 2005; Ernst *et al.*, 2005]. I concentrate on the primary literature on

convection at volcanic passive margins that presents the results of numerical models, paying attention to the parameterization and the starting conditions. I begin with works that resolved significant convection and then mention works dealing with the necking of the lithosphere.

[11] Nielsen and Hopper [2002, 2004] presented self-consistent models for rifting and for convection beneath a rapid change in lithospheric thickness. They imposed nonlinear temperature- and pressure-dependent rheology. They modeled effects of melting and dehydration on density and rheology. They concluded that conditions that produced rapid edge-driven convection also produced rapid convection beneath mature ridges and did not tend to steady state oceanic crustal thickness. They concluded that hot material, like from plumes, was a more likely cause of volcanic margins. They discussed previous modeling efforts that I now summarize.

[12] King and Anderson [1995, 1998] proposed that edge-driven convection produces flood basalts and volcanic margins. King and Ritsema [2000] applied the results to passive margins in the South Atlantic. King [2005] applied the results to the North Atlantic region. This set of models imposed high viscosity continental lithosphere against thinner oceanic lithosphere (Figure 1c). The deeper mantle was initially adiabatic. The non-lithosphere mantle and the lithosphere mantle were each iso-viscous. Viscosity did not advect with the flow nor change with temperature. These models showed strong convection along the margin.

[13] Ghods [2002] imposed nonlinear rheology in his models. The models showed thickened crust near the margin but did not approach steady state crustal thickness at the mature ridge.

[14] Pysklywec and Shahnas [2003] and Shahnas and Pysklywec [2004] included mildly temperature-dependent viscosity in their models. They imposed an initial superadiabatic thermal gradient across the sublithospheric mantle in their models. They obtained vigorous convection around the end of their model continent.

[15] Other models did not follow rifting to the formation of a wide ocean basin. Boutilier and Keen [1999] and Keen and Boutilier [2000] modeled the flow of material into the region of thin lithosphere at a rift margin. They included hot material in some of their models. They obtained only feeble convection. van Wijk *et al.* [2001] and Huisman *et al.* [2001] modeled necking of litho-

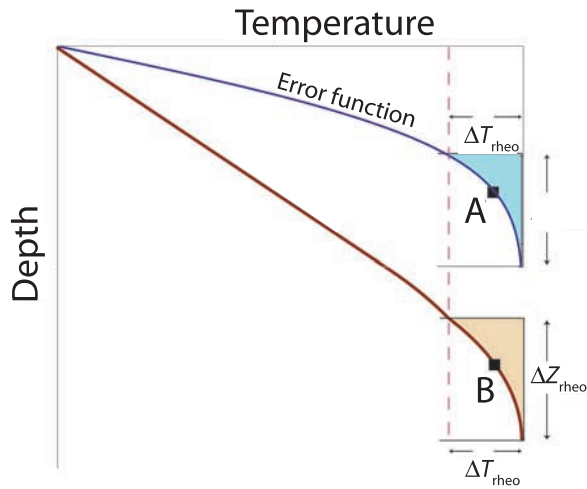


Figure 2. Schematic diagram of the error function geotherm within oceanic lithosphere and the conductive geotherm with stable cratonal lithosphere. The temperature contrast ΔT_{rheo} across the rheological boundary layer depends on the material property T_{η} and is the same for both geotherms. The thickness of the rheological boundary layers is the same even though the surface heat flow is greater in the young oceanic lithosphere than the continent. The temperature difference from the mantle adiabat within the rheological boundary layer is available to drive convection. The thermal gradient within the boundary at points A and B scales with the surface thermal gradient. Note that the thermal boundary layer formed by stretching continental lithosphere [McKenzie, 1978] is thinner than for oceanic lithosphere of the same thickness. One obtains a stretched geotherm by linearly reducing the depth axis of the continent geotherm.

sphere at a rift margin. They included temperature-dependent rheology. Hot underlying material ascended into their model rift. Their models did not explicitly include the sublithospheric asthenosphere and thus could not resolve convection within that region.

3. Heat and Mass Transfer Near the Base of the Lithosphere

[16] Nielsen and Hopper [2002, 2004] illustrated the basic point that conditions that favor vigorous edge-driven convection also favor vigorous convection away from edges. However, the rheology of their models is complex. I retreat to linear purely temperature-dependent rheology for simplicity to obtain simple scaling relationships. I apply the formalism of stagnant-lid convection. I begin by comparing the geotherm beneath stable continental crust with that within oceanic lithosphere.

3.1. Comparison of Continental and Ocean Lithosphere Geotherms

[17] The conductive geotherm through continental regions that have been stable for some time is in quasi-steady state with the heat supplied from below by stagnant-lid convection. Ignoring radioactive heat generation and variations of thermal conductivity with depth for simplicity, the geotherm is linear with depth within the rigid upper part of the lithosphere (Figure 2). The rheological boundary layer lies beneath the rigid lithosphere. Material within this region convects. The geotherm is convective at the top of the layer and adiabatic at its base. The geotherm is adiabatic within the underlying asthenosphere.

[18] In contrast, oceanic lithosphere cools as it ages (Figure 2). Convection at its base replenishes only a fraction of the heat lost from its top. It is thus useful to approximate heat transfer with conductive cooling of an initially hot half-space. This simplification applies as shown in the next subsection for sufficiently young lithosphere. A rheological boundary layer with some convection and some conduction occurs between the rigid overlying lithosphere and the adiabatic underlying asthenosphere.

[19] I compile the well-known half-space conduction formulas with this application in mind. The half-space temperature as a function of depth is

$$T = T_L \operatorname{erf} \left[\frac{z}{\sqrt{4\kappa t_L}} \right], \quad (1)$$

where T is relative to the surface temperature, T_L is the half-space temperature of material at the ridge axis, z is depth, κ is thermal diffusivity, and t_L is lithospheric age [Turcotte and Schubert, 1982, p. 161]. The half-space heat flow as a function of depth is

$$q = k \frac{\partial T}{\partial z} = \frac{kT_L}{\sqrt{\pi\kappa t_L}} \exp \left[\frac{-z^2}{4\kappa t_L} \right] = q_S \exp \left[\frac{-z^2}{4\kappa t_L} \right], \quad (2)$$

where, k is thermal conductivity, and q_S is the surface heat flow [Turcotte and Schubert, 1982, p. 161].

3.2. Stagnant-Lid Convection Formalism

[20] Sleep [2002] gave criteria for when “secondary” convection in the boundary layer at the base of oceanic lithosphere is sufficiently vigorous to

locally perturb the conductive results in (1) and (2). I consider linear (Newtonian) rheology for simplicity. First, the temperature at the top of the rheological boundary layer is less than the half-space temperature T_L by

$$\Delta T_{\text{rtheo}} = 2.4 T_\eta, \quad (3)$$

where T_η is the temperature to change the viscosity by a factor of e [Solomatov and Moresi, 2000]. To maintain generality for arbitrary starting conditions, I let the thickness of the rheological boundary layer be a free parameter. The stresses within the rheological boundary layer scale with the product of its density contrast with the underlying mantle and its thickness, dimensionally,

$$\tau \approx \rho g \alpha \Delta T_{\text{rtheo}} \Delta Z_{\text{rtheo}} \approx \rho g \alpha T_\eta \Delta Z_{\text{rtheo}}, \quad (4)$$

where ρ is density, g is the acceleration of gravity, and α is the volume thermal expansion coefficient. The dimensional form of (3) $\Delta T_{\text{rtheo}} \approx T_\eta$ compacts notation in the second approximate equality. The velocity within the boundary layer is dimensionally the product of the stress and the thickness of the rheological layer divided by the viscosity of the underlying half-space.

$$V \approx \frac{\tau \Delta Z_{\text{rtheo}}}{\eta} \approx \frac{\rho g \alpha T_\eta \Delta Z_{\text{rtheo}}^2}{\eta} \quad (5)$$

The convective heat flow is the product of the volume heat capacity, the temperature contrast (dimensionally T_η), and the velocity

$$q_v \approx \rho C T_\eta V \approx \frac{\rho C \rho g \alpha T_\eta^2 \Delta Z_{\text{rtheo}}^2}{\eta} \quad (6)$$

where the volume specific heat ρC is the product of the isobaric specific heat and the density.

[21] Equation (6) yields the expected steady state result. At steady state, conduction and convection transport comparable amounts of heat around the mid-depth of the rheological boundary layer. This implies that the thermal gradient in the rheological boundary layer is crudely 1/2 the thermal gradient in the overlying conductive lithosphere. Dimensionally

$$q_{ss} \approx k \frac{T_\eta}{\Delta Z_{\text{rtheo}}} \approx \frac{\rho C \rho g \alpha T_\eta^2 \Delta Z_{\text{rtheo}}^2}{\eta}. \quad (7)$$

Solving for ΔZ_{rtheo} yields the well-known parameterized convection relation for quasisteady state in a linear fluid beneath a stagnant lid

$$q_{ss} = 0.47 k T_\eta^{4/3} \left[\frac{\rho g \alpha}{\kappa \eta_H} \right]^{1/3}, \quad (8)$$

and η_H is the viscosity of the adiabatic half-space and the factor 0.47 was obtained by laboratory experiments [Davaile and Jaupart, 1993a, 1993b].

3.3. Convection Beneath Young Lithosphere

[22] Sleep [2002] showed that (6) provides simple relationships for the vigor of stagnant-lid convection beneath young oceanic lithosphere. From (1), the depth to the base of the lithosphere defined by a geotherm has the form

$$Z_L = a_L \sqrt{\kappa t_L}, \quad (9)$$

where a_L is a dimensionless parameter. The thickness of the rheological boundary layer is a fraction of the lithosphere thickness

$$\Delta Z_{\text{rtheo}} = a_R \sqrt{\kappa t_L}, \quad (10)$$

where $a_R \ll a_L$ is another dimensionless parameter. Combining (10) and (6) yields

$$q_v \approx \frac{\rho C \rho g \alpha T_\eta^2 a_R^2 \kappa t_L}{\eta} = \frac{\rho g \alpha T_\eta^2 a_R^2 \kappa t_L}{\eta}, \quad (11)$$

which implies that the convective heat flow increases linearly with age. The thermal time constant for steady state lithosphere is a natural scale [Choblet and Sotin, 2000]. Sleep [2002] conveniently defined it as the time where the conductive heat flow in (2) extrapolates to the steady state heat flow in (8),

$$t_{ss} \equiv \frac{k \rho C T_L^2}{\pi q_{ss}^2}. \quad (12)$$

Combining (8), (11) and (12) with some algebra yields

$$q_v = a_t q_{ss} \frac{t_L}{t_{ss}}, \quad (13)$$

where a_t is a dimensionless parameter obtained from numerical experiments [Sleep, 2002]. Equation (13) applies when it predicts less than the steady state heat flow and in the physically realistic case of strong perturbations as opposed to linear stability

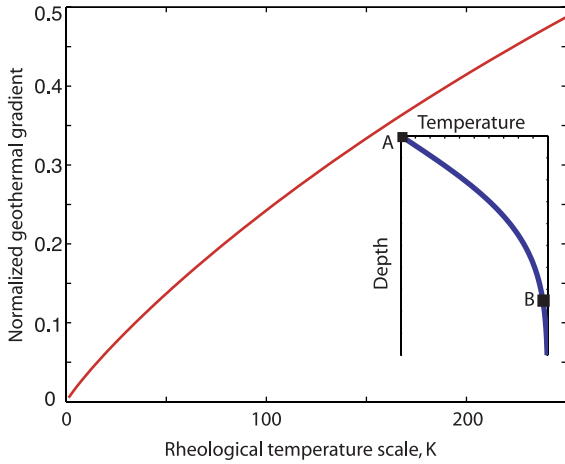


Figure 3. The ratio of the thermal gradient at the center of the thermal boundary layer (point B, inset) to the surface thermal gradient (point A) is shown as a function of the rheological temperature scale, T_η . Point B is in the middle of the rheological boundary layer at $1.2 T_\eta$. The graphs use error function solution in (1) and (2). The temperature access scales linearly with the assumed value of the temperature contrast across the lithosphere, 1300 K; the graph is independent of other physical parameters.

from an infinitesimal perturbation. The heat flow in (13) partitions the behavior of convection into two domains. For times less than t_{ss}/a_t heat flow scales linearly with age and the lithosphere rapidly thickens. For longer times, the heat flow is crudely the steady state heat flow and the lithosphere gradually approaches steady state.

[23] Numerical models calibrate the constant a_t in (13). It is $1/0.27$ and $1/0.50$ for $T_\eta = 60$ K and 120 K, respectively [Sleep, 2002]. This variation occurs because the convective heat flow depends on the thickness of the rheological boundary layer in (6). This property arises as the heat flow and thermal gradient in the rheological boundary layer are less than they are at the surface. The effect is greatest when the rheological temperature contrast is small. For illustration, I let the temperature at the middle of the boundary layer (where the temperature in (1) is $1.2 T_\eta$ less than the half-space temperature) represent the base of the lithosphere in (9). I let the inverse of the conductive half-space heat flow in (2) provide a scaling for the thickness of the rheological boundary layer. The relationship between these parameters is close to linear over the range of interest (Figure 3). (Mathematically, the argument y of the error function in (1) does not

vary much in the parameter space of interest. It is 1.05 and 1.56 for $T_\eta = 150$ and 30 K, respectively. See equation (7.1.23) of Gaultschi [1965]: $\sqrt{\pi} \operatorname{erfc}(y) \rightarrow y \exp(-y^2)$ for large y ; the function is within 25% of the limit for $y = 1$. Thus the ratio of the complementary error function (temperature change) and its derivative (thermal gradient) does not change much in the figure.) Interpolating $1/a_t$ from 0.50 at $T_\eta = 120$ K toward 0 at $T_\eta = 0$ is reasonable for quick estimates from (13). This gives 0.25 at $T_\eta = 60$ K, which is close to the calibrated value of 0.27.

3.4. Application to Convection Beneath Undulant Lithosphere

[24] The formalism of stagnant-lid convection is a subset of boundary layer theory. The thickness of the rheological layer ΔZ_{rheo} is a small fraction of the depth of the convecting system. The base of the lithosphere easily satisfies this requirement in the Earth's mantle. The key inference is that the properties of the boundary layer and not the thickness of the whole system determine the laterally averaged heat flow. That is, cool material once detached from the boundary layer sinks to great depth.

[25] Thus one may need to consider only the local properties of an undulating boundary layer beneath lithosphere of undulating thickness. I infer that the effects are small after the initial instability by noting that only the local thickness of the boundary layer appeared in my derivations. In these scalings, the heat flow in (6) is the dimensional product of the potential gravitational energy per area for material to sink through the boundary layer

$$W = \rho g \alpha T_\eta \Delta Z_{\text{rheo}}^2, \quad (14)$$

and the excess heat per unit volume,

$$H = \rho C T_\eta, \quad (15)$$

divided by the viscosity η . The undulating of the base of the lithosphere affects only W . For transient convection after undulations are imposed, heat conducts horizontally as well as vertically from the boundary layer. Thus the laterally averaged thickness of the boundary layer may be somewhat more than it would be in an equivalent half-space. In terms of (10) and (11), the proportionality constant a_R is somewhat larger but the expression still holds dimensionally. This increases the heat flow somewhat above that the non-undulant lithosphere.

[26] The scaling relationships apply to published models that have linear rheology. In particular, models that show pronounced convection beneath a passive margin are not in the stagnant-lid regime. The passive margins in these models serve to localize the initial instability. Vigorous convection would have occurred had the models been started with a flat base to the lithosphere and a small perturbation.

[27] The models by *Pysklywec and Shahnas* [2003] and *Shahnas and Pysklywec* [2004] have a superadiabatic temperature gradient across the entire mantle. This violates the cardinal assumption of stagnant-lid theory that strong laterally extensive superadiabatic thermal gradients exist only within the boundary layers. Gravitational potential energy in the models is thus stored in the mid-mantle rather than the top boundary layer. From (6) and (14), this thick region once perturbed undergoes vigorous convection.

[28] The models of *King and Anderson* [1998] have isoviscous mantle beneath the lithosphere (Figure 1c). Conduction of heat into the overlying lithosphere cools the underlying asthenosphere. Both the thickness of the cooled region of asthenosphere ΔZ_A and the temperature contrast across the asthenosphere ΔT_A increase with time. The derivation of (8) applies to this isoviscous boundary layer with the full temperature contrast in the asthenospheric boundary layer ΔT_A replacing T_η . The thickness of the cool region beneath the model lithosphere and its temperature anomaly grow until convection becomes vigorous enough to balance the heat conducted to the surface. The margin localizes the initial instability.

[29] The models of *Boutillier and Keen* [1999] and *Keen and Boutillier* [2000] have a high viscosity. The minimum viscosity in the model in Figure 5 of *Keen and Boutillier* [2000] implies a steady state convective heat flow of $\sim 1 \text{ mW m}^{-2}$. Flow in their models is driven by the divergence of the spreading plates.

4. Numerical Modeling

[30] The objective of this paper is to obtain simple generalizable features of edge-modulated convection. I thus keep the numerical models simple so that their relationship to my scaling analysis is more evident. The edge-driven convection hypothesis implies that the rate of flow in the melting zone is a factor of 3 greater than that implied by the

kinematics of diverging lithosphere. Two-dimensional models thus suffice to appraise my inferences from scaling and to verify that they are basically correct.

4.1. Numerical Techniques and Model Parameters

[31] I use the simple material properties that arose in the dimensional analyses in section 3. A cardinal assumption of stagnant-lid formalism is that viscosity depends strongly on temperature so that the thickness of the rheological boundary layer is a small fraction of the thermal thickness of the lithosphere. The exponential form,

$$\eta = \eta_H \exp\left[\frac{\Delta T}{T_\eta}\right], \quad (16)$$

has the virtue of having only two easily understood parameters: η_H the viscosity at the mantle adiabat and temperature scale T_η ; ΔT is the temperature below the mantle adiabat. I did not vary material parameters that are reasonably enough constrained so that scaling relationships suffice to generalize from the models. The thermal conductivity is $3 \text{ W m}^{-1} \text{ K}^{-1}$; the density is 3400 kg m^{-3} ; the temperature scale for viscosity is 60 K; the thermal expansion coefficient is $3 \times 10^{-5} \text{ K}^{-1}$; the volume specific heat is $4 \text{ MJ m}^{-3} \text{ K}^{-1}$, and the acceleration of gravity is $9.8 \text{ m}^2 \text{ s}^{-1}$. The potential temperature of the mantle adiabat is 1300°C . The numerical code is that used by *Sleep* [2002] with minor modifications to input initial conditions and to output results.

[32] The (two-dimensional stream function with over-relaxation) numerical technique follows that of *Andrews* [1972] and *Sleep* [1975]. The models have a uniform 5-km square grid with 1500-km horizontal and 500-km vertical dimensions.

[33] Simple boundary conditions do not impose unnecessary complexity. Boundary conditions for temperature are (artificially) no horizontal heat flow at the sides, (naturally) constant temperature (0°C) at the top, and (artificially) constant temperature (the mantle adiabat (1300°C)) at the bottom. The stream function is set to zero at the top. The velocity and its integral the stream function are hence essentially zero within the very viscous the upper part of the model lithosphere. I impose artificial boundary conditions of no horizontal material flow, no horizontal heat flow, and no vertical shear traction at the side boundaries.

[34] The artificial basal boundary condition is essential for isolating the effects of the boundary layer from those of the rest of the mantle. Mathematically, the first and third derivatives of the stream function perpendicular to the boundary and the first derivative of viscosity equal to zero. This “permeable” boundary condition allows fluid at the mantle adiabat to enter the domain by flowing vertically and dense material to sink out of the domain. A desirable effect of this boundary condition is that the boundary does no work on the rest of the model [Sleep, 1975; Moore *et al.*, 1998].

[35] The half-space temperature beneath the boundary layer thus does not evolve over time. In contrast, the underlying mantle cools over time in models where downwelling material does not escape from the domain of calculation. This increases the half-space viscosity and decreases the stagnant-lid heat flow. Models by Korenaga and Jordan [2003] and Morency *et al.* [2005] have this feature. Although the sublithospheric temperature may actually decrease as oceanic lithosphere ages, this feature makes comparison of model results with scaling results more complicated. A hot basal boundary as in the models of Huang and Zhong [2005] eventually drives convective upwellings heated from below. This happened to some extent in the models of Nielsen and Hopper [2002, 2004].

[36] I let viscosity, the least constrained parameter, be either 10^{18} or 10^{19} Pa s. The latter viscosity represents the domain in (13) where the predicted heat flow for oceanic crust is far from the steady state limit. It approaches the limit of 16.9 mW m^{-2} in 194 Ma. Physically the limit implies equilibrium between the heat flow through stable cratons, 17–25 mW m^{-2} [Rudnick and Nyblade, 1999] and stagnant-lid convection at their base. Oceanic lithosphere would continue to thicken if it escaped subduction and the effects of plumes. The predicted steady state stagnant-lid heat flow cannot be much lower than this without conflicting the ~ 200 -km cratonic lithosphere thickness from xenolith geotherm studies. The former viscosity represents the domain where convective heat flow has approached the steady state limit in (13), here 36.4 mW m^{-2} in 42 Ma. On the Earth, it represents the heat flow through older seafloor ($\sim 40 \text{ mW m}^{-2}$), which implies old oceanic lithosphere approaches steady state balance [Davaille and Jaupart, 1994; Doin *et al.*, 1997; Doin and Fleitout, 2000; Dumoulin *et al.*, 2001]. The predicted steady state stagnant-lid heat flow cannot be much larger than this with

conflicting with the observed subsidence and thickening of young oceanic lithosphere.

[37] Circulation of the mantle through the melting zone for normal MORB can occur only beneath very thin lithosphere because conduction quickly cools it. For example, extensive melting begins at ~ 56 -km depth in the petrological grid of Klein and Langmuir [1987] and Klein [2003]. I let the depth in (9) to the middle of the rheological boundary layer where the temperature is $1.2 T_\eta = 72 \text{ K}$ below the mantle adiabat represent cooling that significantly affects convection and melting. For my parameters, this depth is 13.17 km times the square root of age in million years, 18 Ma for 56 km. The heat flow in (13) at that time for a half-space viscosity of 10^{18} Pa s is 15.6 mW m^{-2} , which is a small fraction of the surface heat flow through young lithosphere (107 mW m^{-2} at 18 Ma). The shallower part of the melting zone cools even faster.

4.2. Starting Conditions With Edges

[38] The starting conditions have either gradual or sharp transitions between thick and thin lithosphere. I use the half-space temperature solution in (1) to obtain reasonable initial conditions. From (13), the predicted convective heat flow depends linearly on age. I thus keep the mean age t_0 of the starting lithosphere constant at 49 Ma. I vary the age as a function of distance x from the edge of the model. The equation,

$$t_L = t_0 + \Delta t_L \sin \left[\frac{2\pi Mx}{X} \right], \quad (17)$$

where Δt_L is a perturbation of age, M is an integer, and X is the width of the model domain, 1500 km, provides a smoothly varying initial base of the lithosphere. Fracture zones and passive margins are likely to be abrupt edges between domains of slowly varying lithosphere thickness. The expression

$$t_L = t_0 + \Delta t_L \left| \sin \left[\frac{2\pi Mx}{X} \right] \right|^{1/16} \text{sign} \left[\sin \left[\frac{2\pi Mx}{X} \right] \right] \quad (18)$$

has this property and retains the feature that it leaves the mean lithospheric age unchanged.

[39] For a given lithospheric thickness, the thickness of the rheological boundary layer is greater of lithosphere formed by cooling from above by conduction than lithosphere thinned by extension [McKenzie, 1978] (Figure 2). The heat flow in (6)

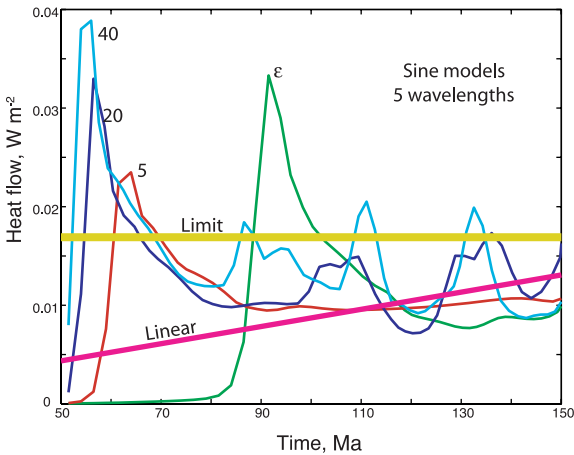


Figure 4. The laterally averaged heat flow for sine models with 5 wavelengths for various initial perturbations. Time is the average age of oceanic lithosphere started at 49 Ma. The numbers of the curves are the perturbation Δt_L in millions of years; ϵ indicates the tiny perturbation of 5000 a. The predicted linear trend in (13) and the stagnant lid limit in (8) are shown for reference. Heat flow increases to a maximum in the initial instabilities and then oscillates about the linear trend.

scales to the thickness of the rheological boundary layer squared. I do not compute models with stretched lithosphere as the heat during their initial convection would be even weaker than that models using the geotherms in (17) and (18).

4.3. Numerical Results

[40] Models with a half-space viscosity of 10^{19} Pa s provide information about the domain where the heat flow from stagnant-lid convection expected from (13) is below its steady state limit. The parameter Δt_L defines the strength of the initial relief of the base of the lithosphere. The age perturbation of 5000 a represents a tiny non-zero perturbation; 5 Ma, 20 Ma, and 40 Ma represent increasingly strong perturbations. I let $M = 5$ represent a rough base of the lithosphere and $M = 2$ represent less rough relief.

[41] Figures 4 and 5 show laterally averaged heat flow as a function of mean lithospheric age. In all the models, heat flow increases in an initial instability. It then slowly decreases toward oscillation about the linear relationship in (13). The “sine” models use the initial condition in (17) (Figures 4 and 5a) and the “box” models use (18) (Figures 5b and 5c).

[42] The suites of models share common features. The instability in the strongly perturbed models grows quickly. The time to instability decreases with the strength of perturbation and the maximum heat flow increases. The heat flow in the models with tiny perturbations gradually increases and convection eventually becomes unstable. The max-

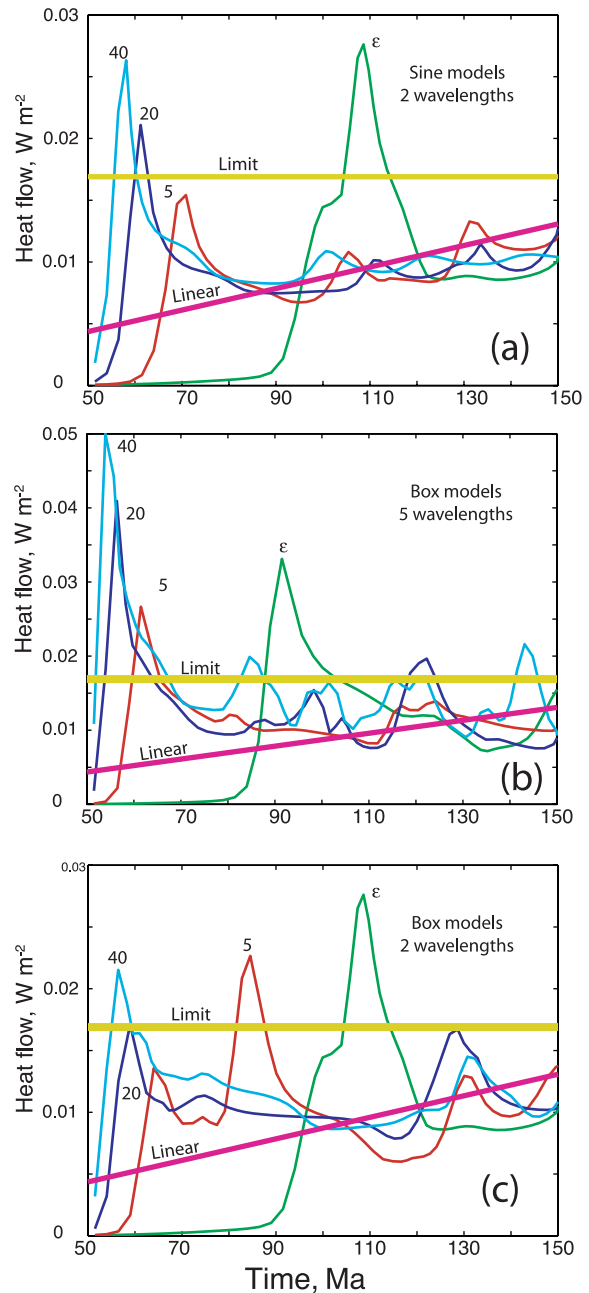


Figure 5. The laterally averaged heat flow for (a) sine models with 2 wavelengths, (b) box models with 5 wavelengths, and (c) box models with 2 lengths. The initial perturbations are the same as in Figure 4. The results are similar to those in Figure 4.

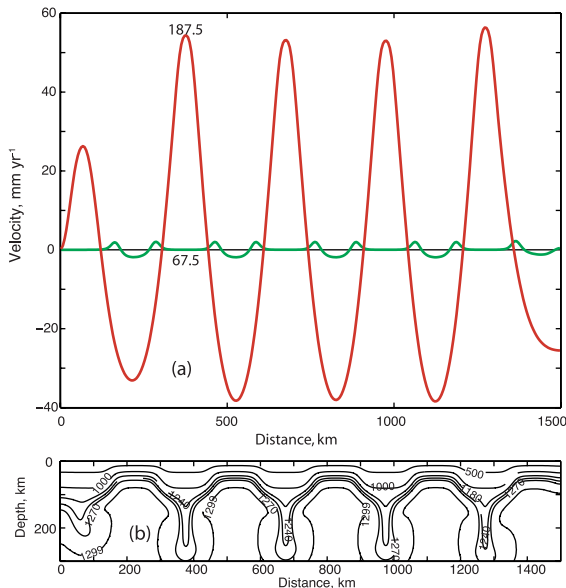


Figure 6. The initial instability at 5 Ma from the start for the box model with 5 wavelengths started with a perturbation of 40 Ma. (a) The vertical velocity at 67.5- and 187.5-km depth is a function of horizontal position. Down is positive. (b) The potential temperature field; contours are 500, 1000, 1180, 1240, 1270, and 1299°C. The velocity is small at shallow depths; the upwelling velocity is less than 1.9 km Ma⁻¹, which slightly augments the volume of material circulated through the melt zone.

imum heat flow is comparable to that in the strongly perturbed models.

[43] The strongly perturbed models with 5 wavelengths (Figures 4 and 5b) show significant oscillations at long times about the predicted linear trend. Models with 2 wavelengths approach the linear trend and have smaller oscillations (Figures 5a and 5c). This implies that the scaling obtained assuming mature stagnant-lid convection in (13) represents the predictable linear increase. It also provides a scale for the magnitude of oscillations and the vigor of starting convection.

[44] Figures 6 and 7 show the vertical velocity at the sublithospheric depth of 187.5 km and the depth of 67.5, which is relevant for melting. The box models have a strong perturbation of 40 Ma so that the young 9 Ma lithosphere is thin enough that upwelling material can melt beneath it. Figure 6 has 5 wavelengths and Figure 7 has 2 wavelengths. The figures show the initial instability 5 Ma after the start of the model.

[45] The “passive” upwelling velocity beneath rifts scales with plate divergence rates, that is, tens of mm a⁻¹ (tens of km Ma⁻¹). The computed convection velocity, however, is much slower than this at 67.5-km depth. *Nielsen and Hopper* [2002, 2004] noted that this feature in their models implies that edge-driven convection is inefficient at circulating material through depths where melting occurs. Rapid flow occurs beneath the lithosphere at 187.5-km depth. In terms of (6), the thickest rheological boundary layer ΔZ_{rheo} and hence the strongest instabilities underlie the thickest lithosphere (Figures 6 and 7). This condition is true for my models where the lithosphere cools slowly from above. It is also true for lithosphere stretched by simple shear as break up margins [*McKenzie, 1978*].

[46] Velocity in (5), like heat flow in (6), scales with the thickness of the rheological boundary layer squared and hence in (13) with plate age. As with laterally averaged heat flow in Figures 4 and 5, this scaling relationship provides a guide to the behavior of the transient start up of convection. The ratio of young to old plate ages is 9/89 = 0.10. The ratio in the velocities at the 2 depths is 1.9/55 = 0.035 and 0.5/33 = 0.015 in Figures 6 and 7, respectively. That is, (5) and (13) actually overestimate the vigor of starting convection beneath the thin young litho-

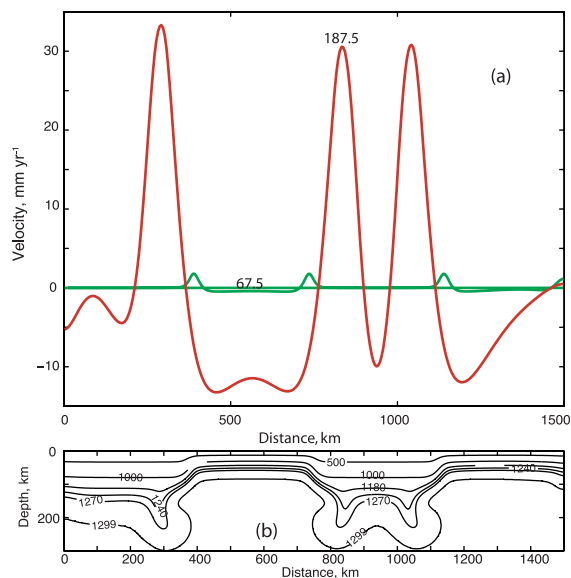


Figure 7. The initial instability at 5 Ma from the start for the box model with 2 wavelengths started with a perturbation of 40 Ma as in Figure 10. Only weak upwelling occurs at the shallower depth; the upwelling velocity is less than 0.5 km Ma⁻¹, which is too small to augment the volume of material circulated through the melt zone.

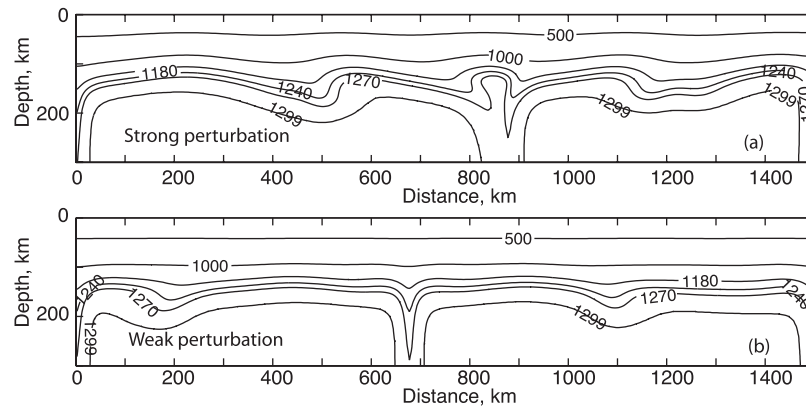


Figure 8. The potential temperature field 101 Ma after the start (150 Ma average age lithosphere) for sine models with 5 wavelengths. (a) Undulations in the base of the lithosphere persist in the model started with the strong perturbation of 40 Ma. (b) The model started with the tiny perturbation retains its flat base to the lithosphere. Both models have mature and nascent downwellings. The vagaries in the formation and persistence of downwellings cause the laterally averaged heat flow to fluctuate over time. The artificial boundary conditions at the sides cause downwellings to persist there.

sphere relative to thick lithosphere. This strengthens the conclusion the convection is weak beneath the thin part of rifts where upwelling material on the MORB adiabat can melt.

[47] Figure 8 compares the thermal state for lithosphere 101 Ma after the start of two sine models with 5 wavelengths. Vigorous convection occurs both in the model started with a strong age perturbation of 40 Ma and the model started from a weak perturbation. The base of the strongly perturbed lithosphere is still undulant. However, the laterally averaged heat flows are similar for the two models (Figure 4). This supports the inference from scaling that undulations do not strongly affect laterally averaged heat flow.

[48] Figure 9 shows heat flow histories for models with a viscosity of 10^{18} Pa s. Strong instabilities occur quickly both for the tiny perturbation and the strong perturbation $\Delta t_L = 40$ Ma. The models then oscillate about predicted steady state. The maximum heat flow is again within a factor of a few of the predicted steady state value for both the strong and the weak perturbation.

[49] These models indicate that a low half-space viscosity as expected from the scaling analysis implies rapid stagnant-lid convection. They do not imply that edge-driven convection is likely to circulate large volumes of material during rift. Initial instabilities form quickly and are short-lived. The velocity during the instability at shallow depths is a fraction of typical plate divergence rates (Figure 10). The total upward motion, however, is limited by the brief duration of the instability.

[50] Comparison of the results in Figure 10 with those of the geometrically equivalent in Figure 7 provides appraisal of the inverse dependence of velocity of viscosity in (5). That is, the velocities in Figure 10 (10 and 400 km Ma^{-1} beneath thin and thick lithosphere) should be a factor of 10 greater than those in Figure 7 (0.5 and 33 km Ma^{-1} beneath thin and thick lithosphere). Again the scaling relationships provide a guide to the behavior of starting convection, especially within the strong downwellings.

[51] Overall, a low “half-space” mantle viscosity implies that grossly unstable regions of thick cool

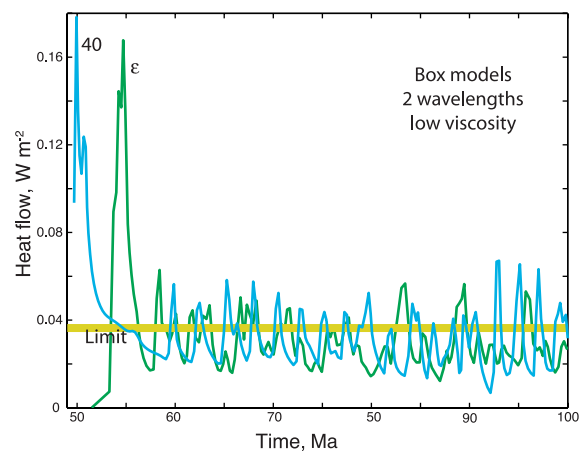


Figure 9. The laterally averaged heat flow for box models with 2 wavelengths for various initial perturbations as in Figure 4. The half-space viscosity is a factor of 10 lower than in the other models. The initial instabilities are brief. Thereafter, the heat flow fluctuates about the stagnant-lid steady state limit.

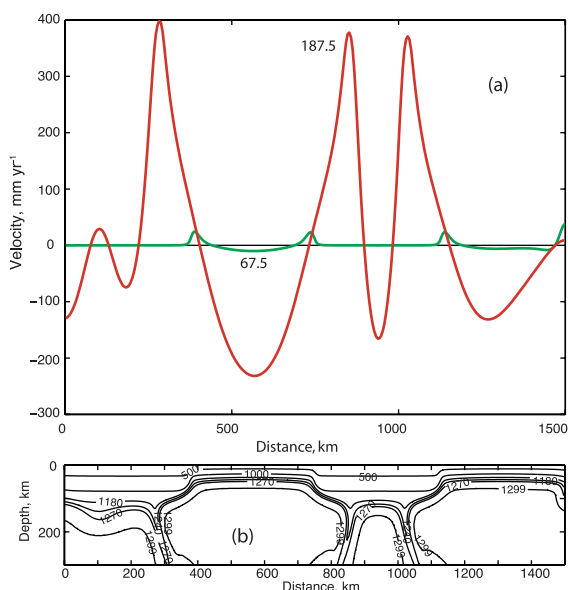


Figure 10. The initial instability at 1 Ma from the start for the box model with 2 wavelengths started with a perturbation of 40 Ma as in Figure 6. The half-space viscosity is a factor of 10 lower than in the other models. Only weak upwelling occurs at the shallower depth; the maximum upwelling velocity is 10 km Ma^{-1} , which moderately augments the volume of material circulated through the melt zone.

rheological boundary layer cannot persist nor build up before or during rifting. Mature stagnant-lid convection is likely everywhere except beneath very young oceanic lithosphere as in the three-dimensional calculations of *Morency et al.* [2005]. Instabilities of already thick boundary layer beneath thick lithosphere are likely to occur early in the rifting process before any highly extended lithosphere exists beneath the nascent margin. These instabilities are thus unlikely to significantly augment melting.

[52] This contrasts with the case of low-viscosity, hot, buoyant plume material. It ponds at the base of the lithosphere storing the flux of a plume tail or a starting plume head. Once rifting commences, the buoyant material flows toward thin lithosphere of the rift where it melts voluminosely.

5. Discussion and Conclusions

[53] Numerical models and the scaling relationships quantify and support the inferences that *Nielsen and Hopper* [2002, 2004] drew from their more complicated models. Edges between thick and thin lithosphere do nucleate instabilities. The laterally averaged heat flow and the flow velocity

during the initial instability depend on the local thickness of the rheological boundary layer. The maximum heat flow during initial instabilities does not depend strongly on the magnitude of the perturbation and is within a factor of a few of the predicted steady state heat flow for mature stagnant-lid convection. The duration of initial instabilities does not depend strongly on the strength of their initial perturbation. Heat flow stabilizes toward that expected for stagnant-lid convection after the initial instability. This is true even when the base of the lithosphere is undulant. Physically, downwelling during the initial instability leaves a thinned rheological boundary layer in its wake, which does not drive subsequent vigorous convection.

[54] Flow during the initial instability does not effectively stir the asthenosphere beneath regions of thin lithosphere. Strong initial downwellings occur beneath thick lithosphere where the rheological boundary layer is thick. The thin rheological boundary beneath thin lithosphere conversely does not drive strong downwelling. There is thus no expectation that realistic edge-convection can increase the total flow at depths where melting occurs by the factor of ~ 3 needed to explain volcanic margins.

[55] For purposes of numerical modeling, one must impose some artificial starting condition unless one does the entire history of the whole Earth. Simple conditions as in my numerical models lead to strong instabilities if the initial thickness of the rheological boundary layer is larger than one in quasi-steady state with stagnant-lid convection. They also lead to the initial downwellings being synchronous. Edges in lithospheric thickness quickly nucleate instabilities. This can lead to the misconception that the edge made the instability quite strong or even that the edge was needed for instability to occur. At a minimum, one must compare models with tiny initial perturbations with those with strong perturbations. My models are intended to illustrate this concept.

[56] Models that follow the evolution of a passive margin through rifting to a mature ocean basin need to allow stagnant-lid convection to become mature before rifting starts. The preexisting convection provides strong perturbations at the time of rifting and prevents overly thick rheological boundary layers from forming. The stagnant-lid convection needs to be self-consistent with the heat flow through the lithosphere. My models covered two attractive limits. (1) The steady state

heat flow is in equilibrium with conductive heat flow through cratons. (2) The steady state heat flow is in equilibrium with heat flow in old ocean basins. In this case, edge-driven convection waxes gradually as lithosphere stretches, rather than producing a large initial instability.

[57] *Nielsen and Hopper* [2002, 2004] included nonlinear viscosity in their models of edge-driven convection that share the features discussed in this section. Dimensional scaling constrains differences and similarities between linear and nonlinear viscosity fluids. The strain rate tensor in a nonlinear isotropic material is

$$\varepsilon'_{ij} = \frac{\tau_{ij}}{2\eta} \left[\frac{\tau}{\tau_{\text{ref}}} \right]^{N-1}, \quad (19)$$

η is a material property with dimensions of viscosity, $|\tau| \equiv 0.5\sqrt{\tau_{ij}\tau_{ij}}$ is the second invariant of the deviatoric stress tensor, and τ_{ref} is a reference stress. (One recovers linear (Newtonian) rheology for $N = 1$.) Dimensional relationships are available for stagnant-lid convection in a nonlinear fluid [*Solomatov*, 1995; *Reese et al.*, 1998, 1999; *Solomatov and Moresi*, 2000; *Sleep*, 2002]. The convective heat flow at steady state is proportional to [*Solomatov and Moresi*, 2000]

$$q_{ss} \propto T_{\eta}^{\frac{2(N+1)}{N+2}} \eta^{\frac{-1}{N+2}}. \quad (20)$$

The temperature contrast of the rheological boundary layer is [*Solomatov and Moresi*, 2000]

$$\Delta T_{\text{theo}} = 1.2T_{\eta}(N+1). \quad (21)$$

The transient heat flow analogous to (6) is [*Sleep*, 2002]

$$q_n = \frac{\rho C T_{\eta} (\rho g \alpha T_{\eta} Z_{\text{theo}})^N Z_{\text{theo}}}{\eta_H \tau_{\text{ref}}^{N-1}}. \quad (22)$$

The heat flow beneath young lithosphere is dimensionally [*Sleep*, 2002]

$$q_b \approx q_{ss} \left[\frac{t_L}{t_{ss}} \right]^{(N+1)/2}. \quad (23)$$

[58] Equation (23) implies that the vigor of convection within a nonlinear fluid cooled from above increases rapidly from negligible to rapid over a brief period of time. Qualitatively, the initial instability is avalanche like. The temperature contrast in the downwelling material in (21) is greater than for

a linear fluid for a given T_{η} . The heat flow for a nonlinear fluid in (22) and the flow velocity depends very strongly on thickness of the rheological boundary layer. The numerical starting conditions for nonlinear rheology are thus much more critical than those in linear rheology models. The heat flow in (23) builds up very slowly before convection becomes quite vigorous. Conversely, the thin rheological layer left after instability needs to thicken over time before it can again drive vigorous convection.

[59] The rheology of the rifting lithosphere needs to be internally consistent with the rheology that governs convection as the stress invariant in (19) includes all macroscopic sources of stress. In the actual Earth, multiple sources of stress interact in a complicated way. Stress sources include local convection, local rifting, drag at the base of plates, and plate boundary forces including “ridge push,” the buoyancy of continental crust and lithosphere, and the buoyancy of plume material contribute to the invariant in (19) and thus interact in a complicated way.

[60] Although *Nielsen and Hopper* [2002, 2004] checked likely parameter space, a highly complex rheology involving melting and dehydration of the volcanic source region and weakening of the lithosphere by intrusions might conceivably be able to produce both volcanic margins and stable ridge axes. One could also make the rheology time dependent [*Solomatov*, 2001]. Very careful attention is needed to starting conditions.

[61] Stagnant-lid formalism combined with sophisticated mineral physics provides a guide for obtaining such candidate rheologies and for generalizing from numerical models. Unless the rheology is exceedingly complicated, it is meaningful to define a rheological boundary layer, more-or-less rigid cool lithosphere, and an underlying half-space. The derivations by *Solomatov and Moresi* [2000] and *Sleep* [2002] and those in this paper carry through. One can include chemical and melt buoyancy along with thermal buoyancy in (4), (14), and (22). One can include the effects of the advection of latent heat as well as specific heat in (6), (15), and (22). One can iteratively apply (21) to obtain a trial temperature contrast across the boundary layer and then evaluate the (effective) power N within the boundary layer. Alternatively, one can follow *Solomatov and Moresi* [2000] and *Sleep* [2002] and obtain the rheological temperature contrast that maximizes heat flow.

[62] Finally, the concept that one should not appeal to highly unstable Earth structures that could not have reasonably persisted applies to models for volcanic passive margins that include large volumes of chemically distinct mantle [e.g., Foulger *et al.*, 2005a, 2005b]. Such hypotheses are too complicated to reject or accept a priori. One needs to show that key features in the models could have remained in the Earth between the time of their formation and the time of rifting. This requires three-dimensional time-dependent calculations from before the origin of the feature, through rifting, to a mature ocean basin.

Acknowledgments

[63] Slava Solomatov and Peter van Keken provided helpful reviews. This research was in part supported by NSF grant EAR-0406658.

References

- Andrews, D. J. (1972), Numerical simulation of sea floor spreading, *J. Geophys. Res.*, *77*, 6470–6481.
- Boutillier, R. R., and C. E. Keen (1999), Small-scale convection and divergent plate boundaries, *J. Geophys. Res.*, *104*, 7389–7403.
- Choblet, G., and C. Sotin (2000), 3D thermal convection with variable viscosity: Can transient cooling be described by a quasi-static scaling law?, *Phys. Earth Planet. Inter.*, *119*, 321–336.
- Davaille, A., and C. Jaupart (1993a), Thermal convection in lava lakes, *Geophys. Res. Lett.*, *20*, 1827–1830.
- Davaille, A., and C. Jaupart (1993b), Transient high-Rayleigh-number thermal convection with large viscosity variations, *J. Fluid Mech.*, *253*, 141–166.
- Davaille, A., and C. Jaupart (1994), The onset of thermal convection in fluids with temperature-dependent viscosity: Application to the oceanic mantle, *J. Geophys. Res.*, *99*, 19,853–19,866.
- Dick, H. J. B., J. Lin, and H. Schouten (2003), An ultraslow-spreading class of ocean ridge, *Nature*, *426*, 405–412.
- Doin, M.-P., and L. Fleitout (2000), Flattening of the oceanic topography and geoid: Thermal versus dynamic origin, *Geophys. J. Int.*, *143*, 582–594.
- Doin, M.-P., L. Fleitout, and U. Christensen (1997), Mantle convection and stability of depleted and undepleted continental lithosphere, *J. Geophys. Res.*, *102*, 2771–2787.
- Dumoulin, C., M.-P. Doin, and L. Fleitout (2001), Numerical simulation of the cooling of an oceanic lithosphere above a convective mantle, *Phys. Earth Planet. Inter.*, *125*, 45–64.
- Ernst, R. E., K. L. Buchan, and I. H. Campbell (2005), Frontiers in large igneous province research, *Lithos*, *79*, 271–297.
- Foulger, G. R., J. H. Natland, and D. L. Anderson (2005a), A source for Icelandic magmas in remelted Iapetus crust, *J. Volcanol. Geotherm. Res.*, *141*, 23–44.
- Foulger, G. R., J. H. Natland, and D. L. Anderson (2005b), Genesis of the Iceland anomaly by plate tectonic processes, in *Plates, Plumes, and Paradigms*, edited by G. R. Foulger *et al.*, *Spec. Pap. Geol. Soc. Am.*, *388*, 595–625.
- Gautschi, W. (1965), Error function and Fresnel integrals, in *Handbook of Mathematical Functions with Formulas, Graphs, and Mathematical Tables, Appl. Math. Ser.*, vol. 55, edited by M. Abramowitz and I. Stegun, pp. 295–329, U.S. Natl. Bur. of Stand., Washington, D. C.
- Geoffroy, L. (2005), Volcanic passive margins, *C. R. Geosci.*, *337*(16), 1395–1408.
- Ghods, A. (2002), Is small scale convection responsible for the formation of thick igneous crust along volcanic passive margins?, *Geophys. Res. Lett.*, *29*(10), 1365, doi:10.1029/2001GL014408.
- Huang, J., and S. Zhong (2005), Sublithospheric small-scale convection and its implications for the residual topography at old ocean basins and the plate model, *J. Geophys. Res.*, *110*, B05404, doi:10.1029/2004JB003153.
- Huismans, R. S., Y. Y. Podladchikov, and S. Cloetingh (2001), Transition from passive to active rifting: Relative importance of asthenospheric doming and passive extension of the lithosphere, *J. Geophys. Res.*, *106*(B6), 11,271–11,291.
- Keen, C. E., and R. R. Boutillier (2000), Interaction of rifting and hot horizontal plume sheets at volcanic rifted margins, *J. Geophys. Res.*, *105*, 13,375–13,387.
- King, S. D. (2005), North Atlantic topographic and geoid anomalies: The result of a narrow ocean basin and cratonic roots?, in *Plates, Plumes, and Paradigms*, edited by G. R. Foulger *et al.*, *Spec. Pap. Geol. Soc. Am.*, *388*, 653–664.
- King, S. D., and D. L. Anderson (1995), An alternative mechanism of flood basalt formation, *Earth Planet. Sci. Lett.*, *136*, 269–279.
- King, S. D., and D. L. Anderson (1998), Edge-driven convection, *Earth Planet. Sci. Lett.*, *160*, 289–296.
- King, S. D., and J. Ritsema (2000), African hot spot volcanism: Small-scale convection in the upper mantle beneath cratons, *Science*, *290*, 1137–1140.
- Klein, E. M. (2003), Geochemistry of the igneous oceanic crust, *Treatise on Geochemistry*, edited by H. D. Holland and K. K. Turekian, vol. 3, edited by R. L. Rudnick, chap. 3.13, pp. 433–463, Elsevier, New York.
- Klein, E. M., and C. H. Langmuir (1987), Global correlations of ocean ridge basalt chemistry with axial depth and crustal thickness, *J. Geophys. Res.*, *92*, 8089–8115.
- Korenaga, J., and T. H. Jordan (2003), Physics of multiscale convection in Earth’s mantle: Onset of sublithospheric convection, *J. Geophys. Res.*, *108*(B7), 2333, doi:10.1029/2002JB001760.
- McKenzie, D. (1978), Some remarks on the development of sedimentary basins, *Earth Planet. Sci. Lett.*, *40*, 25–32.
- Moore, W. B., G. Schubert, and P. Tackley (1998), Three-dimensional simulations of plume-lithosphere interaction at the Hawaiian swell, *Science*, *279*, 1008–1011.
- Morency, C., M.-P. Doin, and C. Dumoulin (2005), Three-dimensional numerical simulations of mantle flow beneath mid-ocean ridges, *J. Geophys. Res.*, *110*, B11407, doi:10.1029/2004JB003454.
- Nielsen, T. K., and J. R. Hopper (2002), Formation of volcanic rifted margins: Are temperature anomalies required?, *Geophys. Res. Lett.*, *29*(21), 2022, doi:10.1029/2002GL015681.
- Nielsen, T. K., and J. R. Hopper (2004), From rift to drift: Mantle melting during continental breakup, *Geochem. Geophys. Geosyst.*, *5*, Q07003, doi:10.1029/2003GC000662.
- Plank, T. M., C. Spiegelman, H. Langmuir, and D. W. Forsyth (1995), The meaning of “mean F”: Clarifying the mean extent of melting at ocean ridges, *J. Geophys. Res.*, *100*, 15,045–15,052.



- Pysklywec, R. N., and M. H. Shahnas (2003), Time-dependent surface topography in a coupled crust-mantle convection model, *Geophys. J. Int.*, *154*, 268–278.
- Reese, C. C., V. S. Solomatov, and L.-N. Moresi (1998), Heat transport efficiency for stagnant lid convection with dislocation viscosity: Application to Mars and Venus, *J. Geophys. Res.*, *103*, 13,643–13,657.
- Reese, C. C., V. S. Solomatov, and L.-N. Moresi (1999), Non-Newtonian stagnant lid convection and magmatic resurfacing on Venus, *Icarus*, *139*, 67–80.
- Rudnick, R. L., and A. A. Nyblade (1999), The thickness and heat production of Archean lithosphere: Constraints from xenolith thermobarometry and surface heat flow, in *Mantle Petrology: Field Observations and High Pressure Experimentation: A Tribute to Francis R. (Joe) Boyd*, edited by Y. Fei, C. M. Bertka, and B. O. Mysen, *Spec. Publ. Geochem. Soc.*, *6*, 3–12.
- Shahnas, M. H., and R. N. Pysklywec (2004), Anomalous topography in the western Atlantic caused by edge-driven convection, *Geophys. Res. Lett.*, *31*, L18611, doi:10.1029/2004GL020882.
- Sleep, N. H. (1975), Stress and flow beneath island arcs, *Geophys. J. R. Astron. Soc.*, *42*, 827–857.
- Sleep, N. H. (2002), Local lithospheric relief associated with fracture zones and ponded plume material, *Geochem. Geophys. Geosyst.*, *3*(12), 8506, doi:10.1029/2002GC000376.
- Solomatov, V. S. (1995), Scaling of temperature- and stress-dependent viscosity convection, *Phys. Fluids*, *7*, 266–274.
- Solomatov, V. S. (2001), Grain size-dependent viscosity and the thermal evolution of the Earth, *Earth Planet. Sci. Lett.*, *191*, 203–212.
- Solomatov, V. S., and L.-N. Moresi (2000), Scaling of time-dependent stagnant lid convection: Application to small-scale convection on Earth and other terrestrial planets, *J. Geophys. Res.*, *105*, 21,795–21,817.
- Turcotte, D. L., and G. Schubert (1982), *Geodynamics: Applications of Continuum Physics to Geological Problems*, 450 pp., John Wiley, New York.
- van Wijk, J. W., R. S. Huismans, M. ter Voorde, and S. A. P. L. Cloetingh (2001), Melt generation at volcanic continental margins: No need for a mantle plume?, *Geophys. Res. Lett.*, *28*, 3995–3998.